energies

Article

Design of Power Location Coefficient System for 6G Downlink Cooperative NOMA Network

Mohamed Hassan [1], Manwinder Singh [1,*], Khalid Hamid [2], Rashid Saeed [3], Maha Abdelhaq [4] and Raed Alsaqour [5]

[1] Department of Wireless Communication, Lovely Professional University, Phagwara 144001, Punjab, India
[2] Department of Communication Systems Engineering, University of Science & Technology, Khartoum P.O. Box 30, Sudan
[3] Department of Computer Engineering, College of Computers and Information Technology, Taif University, P.O. Box 11099, Taif 21944, Saudi Arabia
[4] Department of Information Technology, College of Computer and Information Sciences, Princess Nourah Bint Abdulrahman University, P.O. Box 84428, Riyadh 11671, Saudi Arabia
[5] Department of Information Technology, College of Computing and Informatics, Saudi Electronic University, P.O. Box 93499, Riyadh 93499, Saudi Arabia
* Correspondence: manwinder.2523@gmail.com

Abstract: Cooperative non-orthogonal multiple access (NOMA) is a technology that addresses many challenges in future wireless generation networks by delivering a large amount of connectivity and huge system capacity. The aim of this paper is to design the varied distances and power location coefficients for far users. In addition, this paper aims to evaluate the outage probability (OP) performance against a signal-to-noise ratio (SNR) for a 6G downlink (DL) NOMA power domain (PD) and DL cooperative NOMA PD networks. We combine a DL cooperative NOMA with a 16 × 16, a 32 × 23, and a 64 × 64 multiple-input multiple-output (MIMO) and a 128 × 128, a 256 × 256, and a 512 × 512 massive MIMO in an innovative method to enhance OP performance rate and mitigate the power location coefficient's effect for remote users. The results were obtained from Rayleigh fading channels using the MATLAB simulation software program. According to the outcomes, increasing the power location coefficients for the far user from 0.6 to 0.8 reduces the OP rate because increasing the power location coefficient for the far user decreases the power location coefficient for the near user, which results in less interference between them. In terms of the OP performance rate, the DL cooperative NOMA outperforms the NOMA. According to the findings, the DL cooperative NOMA OP rate outperforms the DL NOMA by a rate of $10^{-0.5}$. Whereas the 16 × 16 MIMO enhances the OP for the far user by 78.0×10^{-4}, the 32 × 32 MIMO increases the OP for the far user by 19.0×10^{-4}, and the 64 × 64 MIMO decreases the OP rate for the far user by 5.0×10^{-5}. At a SNR of 10 dB, the 128 × 128 massive MIMO improves the OP for the far user by 1.0×10^{-5}. The 256 × 256 massive MIMO decreases the OP for the far user by 43.0×10^{-5}, and the 512 × 512 massive MIMO enhances the OP for the far user by 8.0×10^{-6}. The MIMO techniques improve the OP performance, while the massive MIMO technology enhances the OP performance dramatically.

Keywords: non-orthogonal multiple access (NOMA); outage probability (OP); power domain (PD); multiple-input multiple-output (MIMO); 6G network; massive multiple-input multiple-output (MIMO)

check for updates

Citation: Hassan, M.; Singh, M.; Hamid, K.; Saeed, R.; Abdelhaq, M.; Alsaqour, R. Design of Power Location Coefficient System for 6G Downlink Cooperative NOMA Network. *Energies* **2022**, *15*, 6996. https://doi.org/10.3390/en15196996

Academic Editors: R. Maheswar, M. Kathirvelu and K. Mohanasundaram

Received: 27 July 2022
Accepted: 20 September 2022
Published: 23 September 2022

Publisher's Note: MDPI stays neutral with regard to jurisdictional claims in published maps and institutional affiliations.

Copyright: © 2022 by the authors. Licensee MDPI, Basel, Switzerland. This article is an open access article distributed under the terms and conditions of the Creative Commons Attribution (CC BY) license (https://creativecommons.org/licenses/by/4.0/).

1. Introduction

The NOMA has been used to increase the spectral efficiency of mobile next-generation networks [1]. It is one of the most promising technologies for future wireless networking. The primary idea behind NOMA is to serve several users in the same frequency band in the NOMA power domain (PD) [2] but at different power levels, as opposed to the typical orthogonal multiple access (OMA) solutions, such as time-division multiple access (TDMA). The NOMA technology takes advantage of a new dimension in the power field [3].

The NOMA employs successive interference cancellation (SIC), in which one user decodes the other's message from a superposition and then codes the incoming signal before decoding their own. When performing SIC, the near user decodes the information provided by the far user. This is a process that cannot be avoided. Regardless, the close user must decode the data of the far user [4].

Since the near user now has access to the far user's data, he can assist the far user by relaying that data. The close user's retransmission of his data will provide him with diversity because the far user's channel with the transmitting base station (BS) is weak [5]. To present it in another way, he will obtain two copies of the same message. One is from the BS, while the other is a relay from a close user. As a result, the chances of a far user outage should be reduced [6]. The term for this notion is "cooperative communication" or "relaying". Since the close user has access to the data of the far user, the NOMA naturally supports cooperative communication. After all, you are supposed to decode it [7].

When two lines are connected, they convey the same message, which benefits cooperative communication. Even if one connection is down, the other is very certainly operational. Compared to the risk of one link breaking, the chance of both failing simultaneously is extremely unlikely [8].

Due to the increasing importance of fast data transmission and the worldwide expansion of services, significant advances have been achieved in this study area. An alternative method for measuring system effectiveness is spectral efficiency (SE) [9]. One of the most efficient ways to achieve high spectral efficiency is to combine NOMA with MIMO communication, which is a crucial component in designing cellular communication systems. The massive MIMO is a key 6G enabler [10]. By placing many antennas and exploiting the space field to multiplex varied users, the massive-MIMO technology can reduce system latency and deliver incredible communication benefits [11]. A greater spectrum and conductivity improvements are gained when a 6G cooperative NOMA technology is used with a massive MIMO [12].

The system's performance was examined in [13] by analyzing the near–far relay cooperative NOMA system in aiding perfect and imperfect channel state information, imperfect with imperfect SIC over Rayleigh fading channel, but the system is limited in single user situations. The authors of [14] explored the OP in Nakagami-m fading channels and investigated a half-duplex cooperative MIMO NOMA system with incomplete channel state information and SIC. However, the results revealed that no matter how far the user was from the BS, the study treated them all with equal value.

We observe that all previous work has a small number of users and only employs one relay to transmit signals to another user. It is also essential to mention that NOMA systems constantly need power to be allocated to all users because they perform overlapping power domain signals. Since the power assignment correlation coefficients are anticipated to not match, the choice of relay and power allocation is critical for constructing real cooperative NOMA systems.

Motivated by the aforementioned reason, we will investigate the performance analysis of the downlink (DL) NOMA power domain (PD) and the DL cooperative NOMA PD networks. For the sake of simplicity, we simply examine the case of two users, with no regard for interferences from other NOMA users. Our major contributions are summarized as follows:

a. The OPs of a two-user NOMA and a cooperative NOMA system are expressed approximately in closed form via theoretical analyses with different distances and power location coefficients. Additionally, through simulation, we show that the derived OP expressions are more precise than those in [13].
b. We analyzed the findings of OP and impact power location coefficients in the cooperative NOMA system using a 16×16, a 32×23, and a 64×64 MIMO and compared them to our previous results and improvement calculations.

c. We calculated the improved OP performance rate and mitigated the power location coefficient's impact on far users by a cooperative NOMA combined with a 128 × 128, a 256 × 256, and a 512 × 512 massive MIMO.

The remainder of this paper is structured as follows: Section 2 presents the related work. Section 3 discusses the proposed system model. The simulation, parameters, results, and discussion are presented in Section 4. Finally, Section 5 concludes the paper and presents further future work.

2. Related Work

The accurate performance characteristics should be known before implementing a 6G network design to fulfill the system objectives. Several studies offer robust supporting evidence to enhance the transmission circumstances. For instance, in [15], the authors describe a new harmonized dynamic direct and relay detection technique (DD-CDRT) to improve the transmission reliability that uses fully available lateral information to avoid user interference using numerical data to back up the theoretical study and show how the DD-CDRT approach works [16]. At the same time, the proposed broad framework for analyzing NOMA system performance utilizing a two-relaying selection method and spatially random relays has been conducted in [17] and achieved notable outcomes.

Also, the high SNR impact of inadequate user channel gain on dropout performance introduced a new collaborative NOMA protocol for users' DL networks in [18,19]. Hence, according to the remote user's input, the protocol allows the source to adaptively switch between the NOMA direct and the NOMA cooperative transmission modes. The author in [20] applied a remarkable effort via focusing on the cooperative relay selection system with the NOMA's effective resource usage method. Whereas [21] investigated the security of two relay selection approaches for collaborative NOMA systems, resulting in new closed-form equations for the fine and convergent secrecy interruption probability equations [22].

The study in [23] investigated the multiuser detection process for NOMA, which is largely affected by the power distribution of the received signals via the IDMA; the system needs an FEC rate to work properly. Another investigation occurred in [24] and looked at NOMA in which the base station delivers two signals to destinations, obtains OP formulae for two users (close and remote), and emphasizes the role of the close user as a relay. In the same line, the impact of relay considering the direct link has been discussed in [25], but it is better to give more attention to maximizing the received signal.

The NOMA cooperative with simultaneous wireless data and power transfer radio is evaluated in [26]. However, the BS required more respect, as well as added attention to route relaying when transmitting data to two users. Another significant survey in [27] was the performance of a DL NOMA network over Nakagami-m fading channels to assess the OP; the final result demonstrated maximal throughput under varying factors, and the model could be considered to contribute to the development of NOMA systems [28].

3. Cooperative NOMA System Model

In the first scenario, the BS in the DL NOMA PD network with two users, one close to the BS with a strong channel and the other far from the BS with a weak channel, where the distances $(d1,\ d2)$ and power location coefficients $\left(\alpha_n, \alpha_f\right)$ are variables, is illustrated in Figure 1. For the DL cooperative NOMA PD network with two users, one near the BS with a strong channel and the other far from the BS with a weak channel, Figure 2 shows the various distances $(d1,\ d2,\ \text{and}\ d12)$ and power location coefficients $\left(\alpha_n, \alpha_f, \alpha_{nf}\right)$.

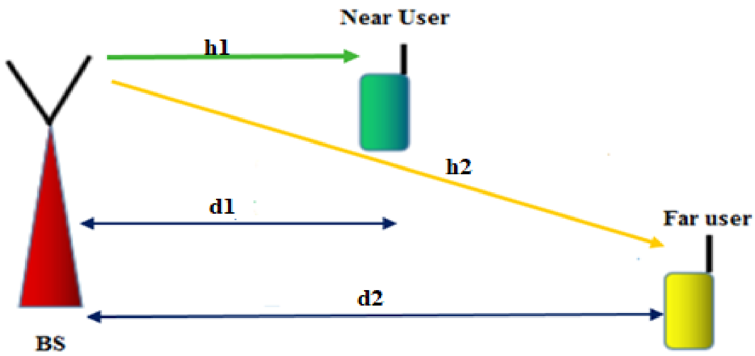

Figure 1. Downlink transmission for the NOMA network.

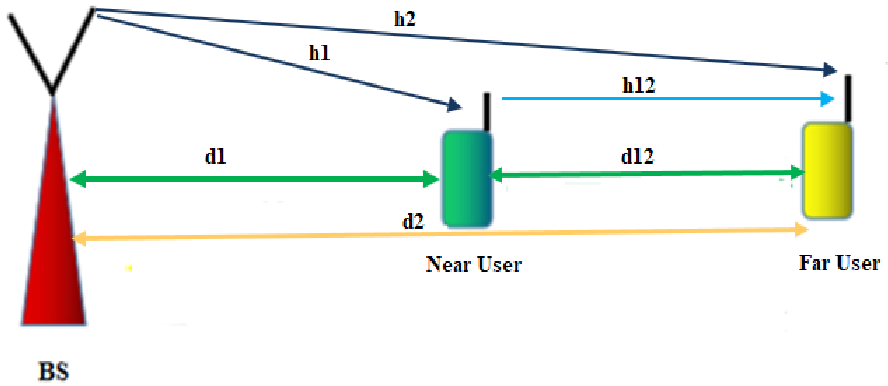

Figure 2. Downlink transmission for the cooperative NOMA network.

In the second case, the NOMA cooperative network is integrated with 16 × 16, 32 × 23, and 64 × 64 MIMO techniques. A similar distance and power location coefficients are used in the first scenario, as it is illustrated in Figure 3.

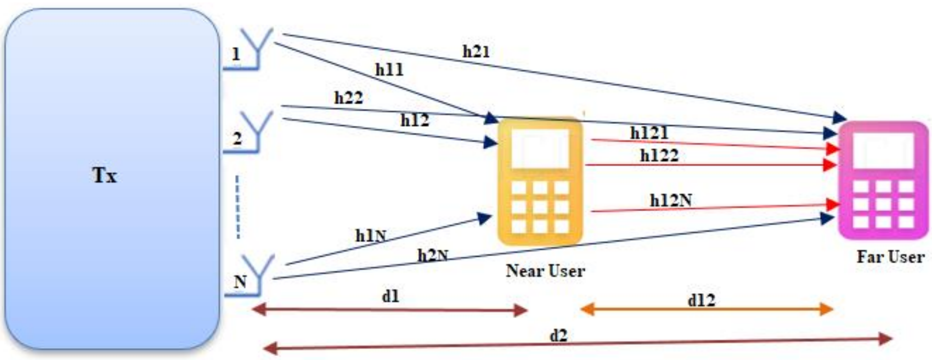

Figure 3. Downlink transmission for the cooperative NOMA network combined with a 16 × 16, a 32 × 23, and a 64 × 64 MIMO.

In the third scenario, the NOMA cooperative network is merged with massive MIMO techniques of 128 × 128, 256 × 256, and 512 × 512. As shown in Figure 4, the distance and power location coefficients employed in the first situation are the same.

In the DL cooperative NOMA, the transmission is divided into two slots [29]. The first slot is referred to as the direct transmission slot, while the second slot is referred to as the relay slot. These slots are used to calculate the total Rayleigh fading channel for each user.

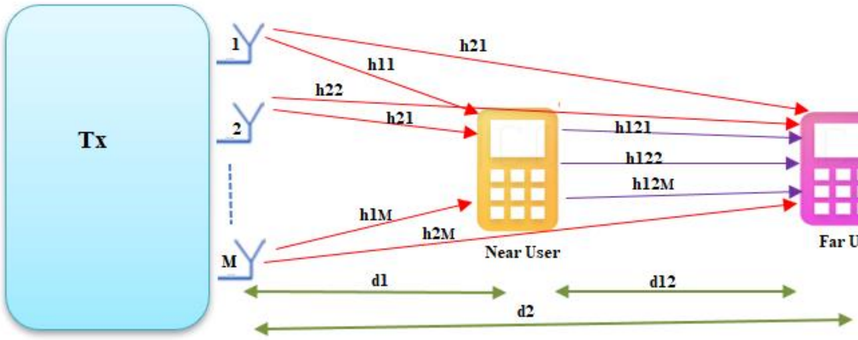

Figure 4. Downlink transmission for the cooperative NOMA network integrated with a 128 × 128, a 256 × 256, and a 512 × 512 MIMO.

The total Rayleigh fading channels for each user are given by [30] and are as follows:

$$h_{fN} = \sum_{f=1}^{N} h_{fN} \tag{1}$$

$$h_{nN} = \sum_{n=1}^{N} h_{nN} \tag{2}$$

where f denotes the far user, n represents the near user, and N indicates the number of antennas.

$N = 1$ is for the DL NOMA and for the DL cooperative NOMA. $N = 16,\ 32,$ and 64 is for the MIMO DL 6G cooperative NOMA. $N = 128,\ 256,$ and 512 is for the massive MIMO DL cooperative NOMA.

3.1. Direct Transmission Slot

The BS transmits data destined for the near user (x_n) and the far user $\left(x_f\right)$ in the direct transmission slot using the NOMA $\left(x_f\right)$. The near user uses SIC to decode the far user's data before decoding their own. The far user does only direct decoding. The possible data rates for the near and far users at the end of the direct transmission slot are given in [30] and are as follows:

$$R_n = \frac{1}{2}\log_2\left(1 + \alpha_n \rho |h_{nN}|^2\right) \tag{3}$$

$$R_{f,1} = \frac{1}{2}\log_2\left(1 + \frac{\alpha_f \rho \left|h_{fN}\right|^2}{\alpha_n \rho \left|h_{fN}\right|^2 + 1}\right) \tag{4}$$

where α_n is the power allocation coefficient for the near user, α_f is the power allocation coefficient for the far user, h_n is the channel between the BS and the near user, h_f is the channel between the BS and the far user. For $SNR = \rho\ /\sigma^2$, ρ is the transmit power and σ^2 is the noise variance. As usual, $\alpha_f > \alpha_n$, and $\alpha_n + \alpha_f = 1$. This is because there are time slots of equal duration; there is a factor of $1/2$ in front of the achievable rates and $R_n,\ R_f$ are the achievable rates during the first time slot alone [31].

3.2. Relaying Slot

The relaying slot is the next half of the time slot. Since the near user decoded the data of the far user in the previous time slot, the near user already has it. The near user simply transmits this data to the far user during the relaying time slot [32]. The far user's achievable rate at the end of the relaying slot is as follows:

$$R_{f,2} = \frac{1}{2}\log_2\left(1 + \alpha_n\rho\left|h_{n\,fN}\right|^2\right) \tag{5}$$

The channel between the near and far users is denoted by h_{nfN}. $R_{f,2} > R_{f,1}$ because of the following two reasons: there is no interference from other transmissions and no fractional power allocation; the far user receives the absolute transmission power [33].

3.3. Diversity Combining

The far user now has two copies of the same information acquired over two distinct routes after the two-time intervals. The far user can now use a diversity-combining approach. For example, utilize selection combining to select the copy with the highest SNR. The far user's achievable rate after the selection combining would be as follows:

$$R_f = \frac{1}{2}\log_2\left(1 + \ max\left(\frac{\alpha_f\rho\left|h_{fN}\right|^2}{\alpha_n\rho\left|h_{fN}\right|^2 \ \ +1}, \ \rho\left|h_{n\,fN}\right|^2\right)\right) \tag{6}$$

If cooperative relaying was not used, the feasible rate of the far user would be calculated as follows:

$$R_{f,noncoop} = \log_2\left(1 + \frac{\alpha_f\rho\left|h_{fN}\right|^2}{\alpha_n\rho\left|h_{fN}\right|^2 \ \ +1}\right) \tag{7}$$

4. Simulation Results and Discussions

After creating a channel gain and computing the outage probability for the far user DL (NOMA, cooperative NOMA, MIMO–NOMA cooperative, and massive MIMO–NOMA cooperative) versus the SNR [34], the system model and simulation parameters were applied in the MATLAB software. Table 1 displays the simulation settings.

Table 1. Simulation Parameters.

Parameters	Values	
Distance	$d_2 = 2d_1$	
SNR	0–25 dB	
Slots	Direct Tx and Relaying slots	
Channel	Rayleigh fading	
Power allocation coefficients	α_f	0.9, 0.8, 0.7, and 0.6
	α_n	0.1, 0.2, 0.3, and 0.4
Path loss exponent	4	
The No. of bits per symbol.	10^6	
MIMO	16 × 16, 32 × 32 and 64 × 64	
Massive MIMO	128 × 128, 256 × 256 and 512 × 512	

Figure 5 shows the OP against the SNR for the two far DL cooperative NOMA PD users with distinct networks at 0.8 and 0.6 power location coefficients, with the findings demonstrating that the OP reduces as the SNR increases. As a result, the OP of the DL 6G cooperative NOMA for the user with a power location coefficient of 0.8 is better than the user with a power location coefficient of 0.6 because it achieves the lowest outage probability at a SNR of 44 dB. In contrast, the user with the lower power location coefficient is more susceptible to interference from the nearby user [35]. Figure 6 depicts the OP vs. the SNR for the DL NOMA PD at 0.8 and 0.6 power location coefficients. The results demonstrate that when the SNR improves, the OP decreases. For the DL NOMA with a power location coefficient of 0.8, the distant user's OP performance rate is identical to that of the 0.6 one until the 10 dB SNR is approached. The analysis results show that the level of performance achieved exceeds the level of the author Z. Ding in [36] by more than 30%.

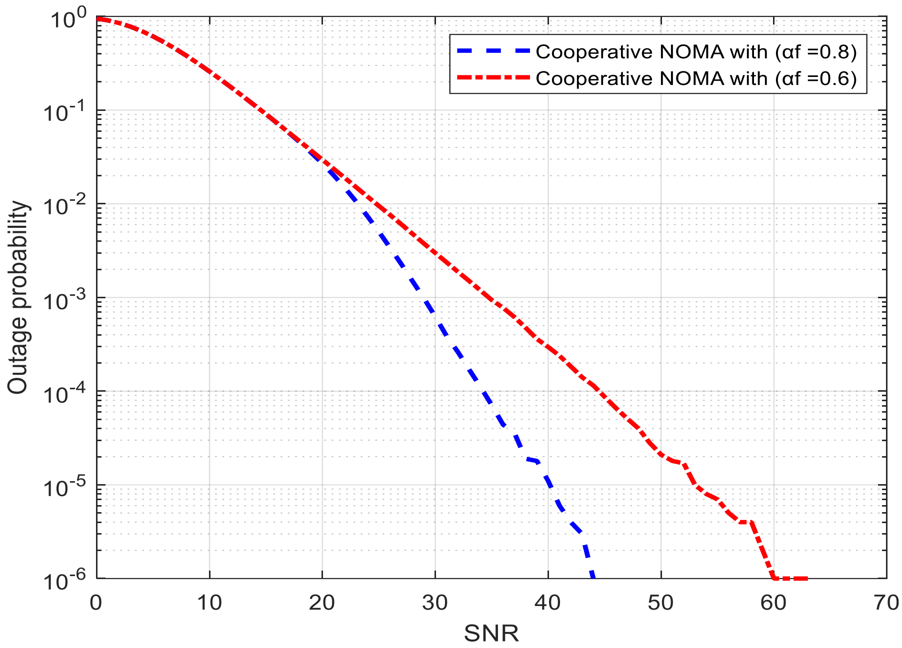

Figure 5. Outage probability against SNR for the two far users' DL cooperative NOMA PD.

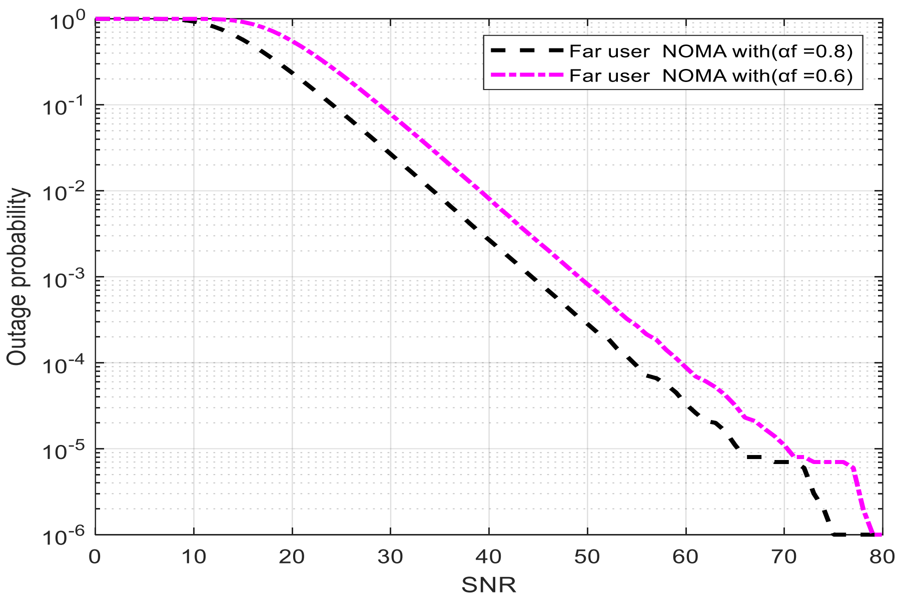

Figure 6. Outage probability against SNR for the two far users' DL NOMA PD.

Figure 7a,b illustrates the OP versus the SNR for the two far users' DL (6G cooperative NOMA and NOMA) PD at 0.9 and 0.7 power location coefficients, respectively. At a SNR of 40 dB, the OP performance at a power location coefficient of 0.7 for the DL cooperative NOMA users is 42.0×10^{-4} times better than the NOMA user. In contrast, the OP performance rate at a power location coefficient of 0.9 for the DL 6G cooperative NOMA user is 4.0×10^{-4} times better than the NOMA user. According to the observations, the DL cooperative NOMA outperforms the NOMA in terms of OP performance rate. Increasing the power location coefficient decreases the OP performance rate because increasing the power location coefficient of the far user decreases the power location coefficient of the near user, resulting in less interference between them. According to the data, the level of performance attained is 10% higher than the level attained in [13,14].

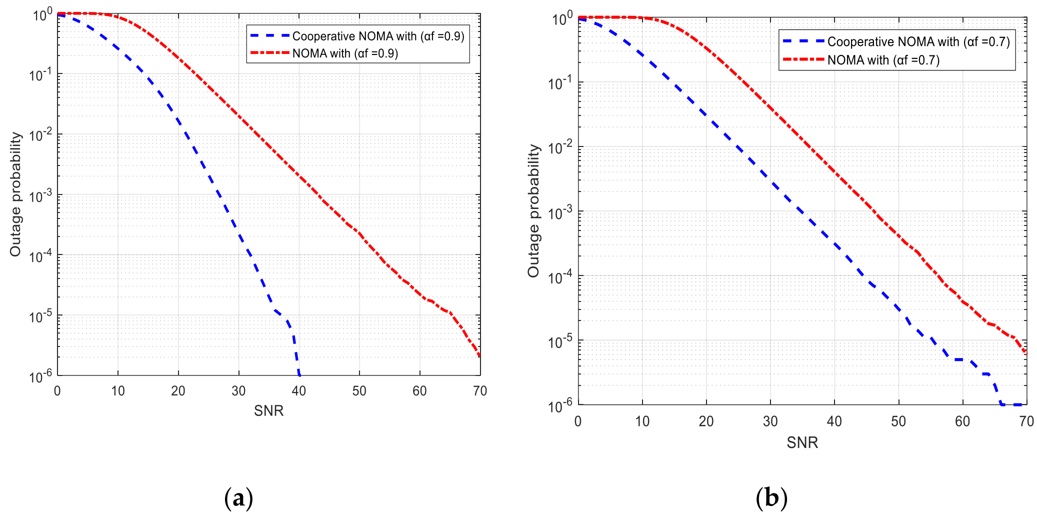

Figure 7. Outage probability against SNR for the two different users' DL NOMA and DL cooperative NOMA. (**a**) α_f = 0.9 (**b**) α_f = 0.7.

Figure 8 shows the OP vs. the SNR at 0.8 power location coefficients for the four varied far users of the cooperative NOMA, the 16 × 16 MIMO cooperative NOMA, the 32 × 32 MIMO cooperative NOMA, and the 64 × 64 MIMO cooperative NOMA [37]. At a SNR of 10 dB, the OP rate for the far user 64 × 64 MIMO cooperative NOMA is 5.0×10^{-4}. In contrast, the OP rate for the far user 32 × 32 MIMO cooperative NOMA is 19.0×10^{-4}. The OP rate for the user 32 × 32 MIMO cooperative NOMA is 78.0×10^{-4}, and the OP rate for the user 6G cooperative NOMA is 8644.0×10^{-4}. The rate of improvement in the OP by the best user using the cooperative 64 × 64 MIMO–NOMA versus the worst user using the cooperative NOMA is 8639.0×10^{-4}. The MIMO technique improves the overall OP performance; the obtained values are 4% higher than the values obtained in [38–40].

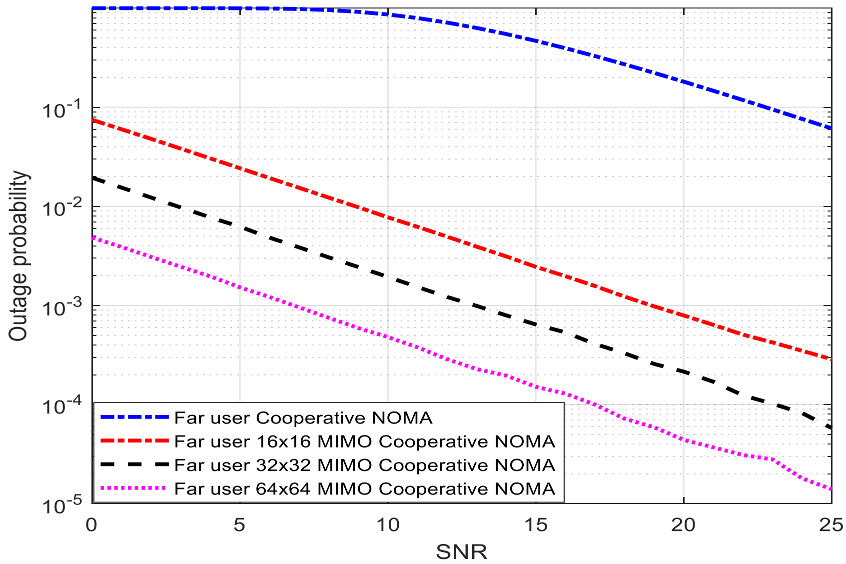

Figure 8. Outage probability against SNR for four different far users (cooperative NOMA and MIMO–cooperative NOMA).

Figure 9 shows the OP against the SNR at 0.8 power location coefficients for the four far users of the cooperative NOMA, the 128 × 128 massive MIMO cooperative NOMA, the

256 × 256 massive MIMO cooperative NOMA, and the 512 × 512 massive MIMO cooperative NOMA [41]. At a SNR of 14 dB, the OP for the far user 512 × 512 massive MIMO cooperative NOMA is 8.0 × 10^{-5}, while the OP for the user 256 × 256 massive MIMO cooperative NOMA is 43.0 × 10^{-5}. The OP for the user 128 × 128 massive MIMO cooperative NOMA is 1.0 × 10^{-5}, and the OP for the user cooperative NOMA is 8644.0 × 10^{-5}. Between the best user utilizing the cooperative 512 × 512 massive MIMO–NOMA and the worst user using the cooperative NOMA, the rate of improvement in the OP is 86432.0 × 10^{-5}. The massive MIMO technique significantly increases the OP's performance. The results show that the achieved performance is better than [42] by 15%.

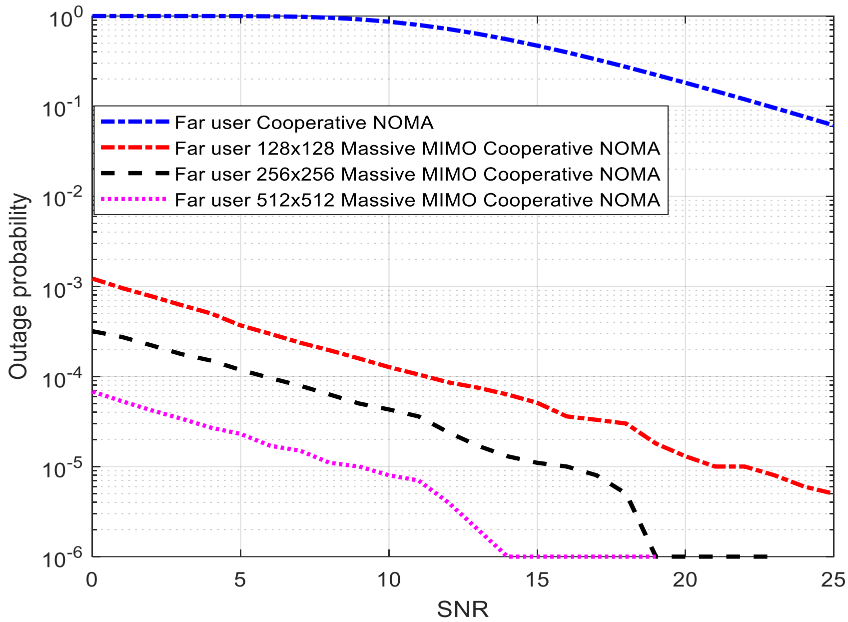

Figure 9. Outage probability against SNR for three different far users (cooperative NOMA, massive-MIMO–NOMA cooperative).

5. Conclusion and Future Work

The influence of distant users' power location coefficients on the DL NOMA PD and the DL cooperative NOMA PD concerning OP against SNR was investigated in this work. Furthermore, we designed and incorporated a MIMO, 16 × 16, 32 × 32, 64 × 64, and massive MIMO, 128 × 128, 256 × 256, and 512 × 512, into the DL cooperative NOMA PD system. The findings show that when the power location coefficients for the far user are increased, the OP performance rate goes down. This is because the power location coefficients for the near user are decreased; therefore, there is less interference between them.

The findings indicate that the OP rate of the DL 6G cooperative NOMA exceeds the DL NOMA by a range of 10–0.5. At a SNR of 10 dB, the 16 × 16 MIMO reduces the OP for the far user by 78.0 × 10^{-4}, the 32 × 32 MIMO decreases the OP for the far user by 16.0 × 10^{-4}, and the 64 × 64 MIMO improves the OP rate for the far user by 5.0 × 10^{-4}. In contrast, the 128 × 128 massive MIMO reduces the OP for the far user by 1.0 × 10^{-5}, the 256 × 256 massive MIMO enhances the OP for the far user by 43.0 × 10^{-5}, and the 512 × 512 massive MIMO improves the OP for the far user by 8.0 × 10^{-6}. The rate of improvement in the OP by the best user using the DL 512 × 512 massive MIMO cooperative NOMA versus the best user using the DL 64 × 64 cooperative NOMA is 492.0 × 10^{-6}.

The massive MIMO technology greatly improves the OP's performance, whereas the MIMO approach improves the OP's performance. In the future, researchers will explore combining the massive MIMO cooperative NOMA with a cognitive radio.

Author Contributions: Conceptualization, M.H.; methodology, M.H. and M.S.; software, M.H.; validation, M.H., M.S. and K.H.; formal analysis, M.H., M.S. and K.H.; investigation, R.S. and R.A.; resources, R.S., M.A. and R.A.; data curation, R.S., M.A. and R.A.; writing—original draft preparation, M.H.; writing—review and editing, M.A., R.S. and R.A.; visualization, M.H. and K.H.; supervision, M.S.; project administration, M.S.; funding acquisition, M.A. All authors have read and agreed to the published version of the manuscript.

Funding: This research was supported by the Princess Nourah bint Abdulrahman University Researchers Supporting Project Number (PNURSP2022R97), Princess Nourah bint Abdulrahman University, Riyadh, Saudi Arabia.

Data Availability Statement: Not applicable.

Acknowledgments: Princess Nourah bint Abdulrahman University Researchers Supporting Project Number (PNURSP2022R97), Princess Nourah bint Abdulrahman University, Riyadh, Saudi Arabia.

Conflicts of Interest: The authors declare no conflict of interest.

References

1. Li, A.; Lan, Y.; Chen, X.; Jiang, H. Non-orthogonal multiple access (NOMA) for future downlink radio access of 5G. *China Commun.* **2015**, *12*, 28–37. [CrossRef]
2. Mukhtar, A.M.; Saeed, R.A.; Mokhtar, R.A.; Ali, E.S.; Alhumyani, H. Performance Evaluation of Downlink Coordinated Multipoint Joint Transmission under Heavy IoT Traffic Load. *Wirel. Commun. Mob. Comput.* **2022**, *2022*, 6837780. [CrossRef]
3. Ahmed, M.A.; Mahmmod, K.F.; Azeez, M.M. On the performance of non-orthogonal multiple access (NOMA) using FPGA. *Int. J. Electr. Comput. Eng.* **2020**, *10*, 2151. [CrossRef]
4. Al-Adwany, M.A. Efficient power allocation method for non orthogonal multiple access 5G systems. *Int. J. Electr. Comput. Eng.* **2020**, *10*, 2139. [CrossRef]
5. Mokhtar, R.A.; Saeed, R.A.; Alhumyani, H. Cooperative Fusion Architecture-based Distributed Spectrum Sensing Under Rayleigh Fading Channel. *Wirel. Pers. Commun.* **2022**, *124*, 839–865. [CrossRef]
6. Budhiraja, I.; Kumar, N.; Tyagi, S.; Tanwar, S.; Han, Z.; Piran, M.J.; Suh, D.Y. A systematic review on NOMA variants for 5G and beyond. *IEEE Access* **2021**, *9*, 85573–85644. [CrossRef]
7. Do, D.-T.; Nguyen, T.-T.T. Impacts of relay and direct links at destinations in full-duplex non-orthogonal multiple access system. *Indones. J. Electr. Eng. Comput. Sci.* **2022**, *26*, 269–277. [CrossRef]
8. Hassan, M.B.; Ali, E.S.; Saeed, R.A. Ultra-Massive MIMO in THz Communications: Concepts, Challenges and Applications. In *Next Generation Wireless Terahertz Communication Networks*, 1st ed.; CRC Press: Boca Raton, FL, USA, 2021; pp. 267–297.
9. Oleiwi, H.; Saeed, N.; Al-Raweshidy, H. Cooperative SWIPT MIMO-NOMA for Reliable THz 6G Communications. *Netw. J.* **2022**, *2*, 257–269. [CrossRef]
10. Fang, F.; Zhang, H.; Cheng, J.; Roy, S.; Leung, V.C. Joint user scheduling and power allocation optimization for energy-efficient NOMA systems with imperfect CSI. *IEEE J. Sel. Areas Commun.* **2017**, *35*, 2874–2885. [CrossRef]
11. Satrya, G.B.; Shin, S.Y. Security enhancement to successive interference cancellation algorithm for non-orthogonal multiple access (NOMA). In Proceedings of the 2017 IEEE 28th Annual International Symposium on Personal Indoor, and Mobile Radio Communications (PIMRC), Montreal, QC, Canada, 8–13 October 2017; pp. 1–5.
12. Li, G.; Mishra, D.; Jiang, H. Cooperative NOMA with incremental relaying: Performance analysis and optimization. *IEEE Trans. Veh. Technol.* **2018**, *67*, 11291–11295. [CrossRef]
13. Singh, S.; Bansal, M. Performance analysis of non-orthogonal multiple access assisted cooperative relay system with channel estimation errors and imperfect successive interference cancellation. *Trans. Emerg. Telecommun. Technol.* **2022**, *32*, e4374. [CrossRef]
14. Srinivasarao, K.; Maruthu, S. Outage analysis of cooperative NOMA system with imperfect successive interference cancellation and channel state information over Rayleigh fading channel. *Int. J. Commun. Syst.* **2022**, in press. [CrossRef]
15. Jaber, Z.H.; Kadhim, D.J.; Al-Araji, A.S. Medium access control protocol design for wireless communications and networks review. *Int. J. Electr. Comput. Eng.* **2022**, *12*, 1711. [CrossRef]
16. Yang, M.; Chen, J.; Yang, L.; Lv, L.; He, B.; Liu, B. Design and performance analysis of cooperative NOMA with coordinated direct and relay transmission. *IEEE Access* **2019**, *7*, 73306–73323. [CrossRef]
17. Hassan, M.B.; Alsharif, S.; Alhumyani, H.; Ali, E.S.; Mokhtar, R.A.; Saeed, R.A. An enhanced cooperative communication scheme for physical uplink shared channel in NB-IoT. *Wirel. Pers. Commun.* **2021**, *120*, 2367–2386. [CrossRef]
18. Dahi, N.; Hamdi, N. Outage performance of generalized cooperative NOMA systems with SWIPT in nakagami-m fading. *J. Commun. Softw. Syst.* **2018**, *14*, 386–391. [CrossRef]
19. Kader, M.F.; Shahab, M.B.; Shin, S.Y. Exploiting non-orthogonal multiple access in cooperative relay sharing. *IEEE Commun. Lett.* **2017**, *21*, 1159–1162. [CrossRef]
20. Elfatih, N.M.; Hasan, M.K.; Kamal, Z.; Gupta, D.; Saeed, R.A.; Ali, E.S.; Hosain, M.S. Internet of vehicle's resource management in 5G networks using AI technologies: Current status and trends. *IET Commun.* **2022**, *16*, 400–420. [CrossRef]

21. Saeed, R.A.; Abbas, E.B. Performance evaluation of MIMO FSO communication with gamma-gamma turbulence channel using diversity techniques. In Proceedings of the 2018 International Conference on Computer, Control, Electrical, and Electronics Engineering (ICCCEEE), Khartoum, Sudan, 12–14 August 2018; pp. 1–5.
22. Han, S.; Chih-Lin, I.; Xu, Z.; Sun, Q. Energy efficiency and spectrum efficiency co-design: From NOMA to network NOMA. *IEEE COMSOC MMTC E-Lett.* **2014**, *9*, 21–24.
23. Lien, S.-Y.; Shieh, S.-L.; Huang, Y.; Su, B.; Hsu, Y.-L.; Wei, H.-Y. 5G new radio: Waveform, frame structure, multiple access, and initial access. *IEEE Commun. Mag.* **2017**, *55*, 64–71. [CrossRef]
24. Luo, S.; Teh, K.C. Adaptive transmission for cooperative NOMA system with buffer-aided relaying. *IEEE Commun. Lett.* **2017**, *21*, 937–940. [CrossRef]
25. Islam, S.R.; Avazov, N.; Dobre, O.A.; Kwak, K.-S. Power-domain non-orthogonal multiple access (NOMA) in 5G systems: Potentials and challenges. *IEEE Commun. Surv. Tutor.* **2016**, *19*, 721–742. [CrossRef]
26. Timotheou, S.; Krikidis, I. Fairness for non-orthogonal multiple access in 5G systems. *IEEE Signal Process. Lett.* **2015**, *22*, 1647–1651. [CrossRef]
27. Manglayev, T.; Kizilirmak, R.C.; Kho, Y.H.; Bazhayev, N.; Lebedev, I. NOMA with imperfect SIC implementation. In Proceedings of the IEEE EUROCON 2017—17th International Conference on Smart Technologies, Ohrid, Macedonia, 6–8 July 2017; pp. 22–25.
28. Manglayev, T.; Kizilirmak, R.C.; Kho, Y.H. Optimum power allocation for non-orthogonal multiple access (NOMA). In Proceedings of the 2016 IEEE 10th International Conference on Application of Information and Communication Technologies (AICT), Baku, Azerbaijan, 12–14 October 2016; pp. 1–4.
29. Nguyen, T.; Do, D.-T. Novel multiple access for cooperative networks with nakagami-m fading: System model and performance analysis. *Indones. J. Electr. Eng. Comput. Sci.* **2020**, *19*, 233–240.
30. Van, H.T.; Vo, T.A.; Le, D.H.; Phu, M.Q.; Nguyen, H.-S. Outage performance analysis of non-orthogonal multiple access systems with RF energy harvesting. *Int. J. Electr. Comput. Eng.* **2021**, *11*, 4135. [CrossRef]
31. Ding, Z.; Peng, M.; Poor, H.V. Cooperative non-orthogonal multiple access in 5G systems. *IEEE Commun. Lett.* **2015**, *19*, 1462–1465. [CrossRef]
32. Abdelrahman, Y.T.; Saeed, R.A.; El-Tahir, A. Multiple Physical Layer Pipes performance for DVB-T2. In Proceedings of the 2017 International Conference on Communication, Control, Computing and Electronics Engineering (ICCCCEE), Khartoum, Sudan, 16–18 January 2017; pp. 1–7.
33. Zhang, Y.; Wang, H.-M.; Yang, Q.; Ding, Z. Secrecy sum rate maximization in non-orthogonal multiple access. *IEEE Commun. Lett.* **2016**, *20*, 930–933. [CrossRef]
34. Zhang, Y.; Wang, H.-M.; Zheng, T.-X.; Yang, Q. Energy-efficient transmission design in non-orthogonal multiple access. *IEEE Trans. Veh. Technol.* **2016**, *66*, 2852–2857. [CrossRef]
35. Ding, Z.; Poor, H.V. Design of massive-MIMO-NOMA with limited feedback. *IEEE Signal Processing Lett.* **2016**, *23*, 629–633. [CrossRef]
36. Ding, Z.; Liu, Y.; Choi, J.; Sun, Q.; Elkashlan, M.; Chih-Lin, I.; Poor, H.V. Application of non-orthogonal multiple access in LTE and 5G networks. *IEEE Commun. Mag.* **2017**, *55*, 185–191. [CrossRef]
37. Liu, Y.; Ding, Z.; Elkashlan, M.; Poor, H.V. Cooperative non-orthogonal multiple access with simultaneous wireless information and power transfer. *IEEE J. Sel. Areas Commun.* **2016**, *34*, 938–953. [CrossRef]
38. Ding, Z.; Fan, P.; Poor, H.V. Random beamforming in millimeter-wave NOMA networks. *IEEE Access* **2017**, *5*, 7667–7681. [CrossRef]
39. Aldababsa, M.; Kucur, O. Outage and ergodic sum-rate performance of cooperative MIMO-NOMA with imperfect CSI and SIC. *Int. J. Commun. Syst.* **2020**, *33*, e4405. [CrossRef]
40. Sanjay, M.; Roy, D.; Kundu, S. Outage analysis for NOMA-based energy harvesting relay network with imperfect CSI and transmit antenna selection. *IET Commun.* **2020**, *14*, 2240–2249. [CrossRef]
41. Wang, Z.; Peng, Z. Secrecy performance analysis of relay selection in cooperative NOMA systems. *IEEE Access* **2019**, *7*, 86274–86287. [CrossRef]
42. Shashank, S.; Muralikrishnan, S.; Sheetal, K. Outage Probability of Uplink Cell-Free Massive MIMO Network with Imperfect CSI Using Dimension-Reduction Method. *arXiv* **2021**. [CrossRef]